

Activation Cross-Section Survey of Deuteron-Induced Reactions*

NORTON BARON† AND BERNARD L. COHEN
University of Pittsburgh, Pittsburgh, Pennsylvania
 (Received 2 November 1962)

A survey was made of activation cross sections for various nuclear reactions induced by 20-MeV deuterons. The (d,p) and (d,t) cross sections increase monotonically with increasing mass number, and in one case (Ni^{68}) the absolute (d,p) cross section is closely predicted by a distorted-wave Born approximation calculation. They are undoubtedly stripping and pickup reactions with little or no compound nucleus contribution. The fact that Coulomb barriers do not affect (d,t) cross sections indicates that the pickup occurs far outside the nucleus. The cross sections for $(d,2p)$ reactions are consistent with a model wherein the second proton is "evaporated" from a compound nucleus, but the level density parameters needed to fit this theory are somewhat lower than expected; this may indicate a contribution from a mechanism in which both protons are emitted in a direct interaction. Excluding the lightest element studied, Cl^{35} , the $(d,p\alpha) + (d,\alpha p)$ activation cross sections are consistent with calculations assuming a reaction path that is predominantly $(d,p\alpha)$ with evaporation of the second particle (i.e., one alpha) from a compound nucleus; however the reaction on Cl^{35} seems to proceed by the path $(d,\alpha p)$ with both particles being evaporated. Cross sections for $(d,2n)$ and $(d,n\alpha)$ reactions in the mass range 60 to 90 indicate that many more low-energy neutrons than low-energy protons are emitted as first particles in deuteron-induced reactions; this indicates that compound nucleus formation is more important than stripping in these reactions.

A SURVEY experiment was undertaken to determine the activation cross sections for several different deuteron-induced nuclear reactions. The purpose was to obtain information concerning the reaction mechanism by noting the occurrence of systematic cross-section variations and to determine the parameters in theories that seem pertinent for a particular reaction. In addition, activation cross sections are often useful in nuclear technology.

EXPERIMENTAL PROCEDURES

The deuteron bombardments were conducted at the Lewis Research Center of the National Aeronautics and Space Administration in Cleveland, Ohio. This laboratory kindly allowed the authors to use their 60-in. cyclotron for the necessary bombardments; the deuteron energy produced by this cyclotron is 21.5 MeV. The analyses of the activated targets were made at the Radiation Laboratory of the University of Pittsburgh.

Because of limited access to the deuteron beam, it was considered more desirable for an initial survey experiment of this type to measure activation cross sections for as many different reactions as possible, within a narrow range of incident deuteron energies, instead of measuring comparatively few excitation functions. Consequently, a stack of about nine different targets was positioned in the path of the deuteron beam for each bombardment. This resulted in a difference of incident deuteron energies of about 22 MeV between the first and last targets in the stack. Each target stack was subjected to an irradiation of approximately 4500 μC .

The activation cross sections were determined by

* This work was done at Sarah Mellon Scaife Radiation Laboratory and supported by the National Science Foundation and the Office of Naval Research.

† Present address: Lewis Research Center, National Aeronautics and Space Administration, Cleveland, Ohio.

comparison beta counting. In general, each bombardment was monitored by a thin aluminum foil at the head of the target stack, immediately followed by a bismuth target, and finally a bismuth target at the rear of the stack. The monitor reactions^{1,2} used were

$${}_{13}\text{Al}_{14}^{27}(d,\alpha p){}_{11}\text{Na}_{13}^{24}, \quad T_{1/2} = 15 \text{ h}$$

and

$${}_{83}\text{Bi}_{126}^{209}(d,p){}_{83}\text{Bi}_{127}^{210}, \quad T_{1/2} = 5 \text{ days.}$$

The experimental arrangement for measuring the beta activity consisted of six typical Lucite-lined lead shields having 1½-in.-thick walls. In each shield was housed an end window Geiger-Mueller tube having a mica window 1.9 mg/cm² thick. The counting tubes used were Tracerlab TGC-2 self-quenching G-M tubes. The output from each G-M tube was fed into a scaler which, after accumulating a preset number of counts, drove a pen on a 10-pen Esterline-Angus strip chart recorder. An analysis of the strip chart then allowed one to plot the observed decay rate as a function of time, from which the half-life of the reaction product could be measured. Cross sections of competitive reactions whose products have different atomic numbers but similar half-lives were measured by the above procedure after performing standard radiochemical separations. The radiochemical procedures used in this work were taken from standard references.³⁻¹⁶

¹ P. A. Lenk and R. J. Slobodrian, *Phys. Rev.* **116**, 1229 (1959).

² W. J. Ramler, J. Wing, D. J. Henderson, and J. R. Huizenga, *Phys. Rev.* **114**, 154 (1959).

³ J. A. Corbett and C. J. L. Lock, Canadian Atomic Energy Commission Report, UKE-CR-1003, April, 1958 (unpublished).

⁴ G. Friedlander and J. W. Kennedy, *Nuclear and Radiochemistry* (John Wiley & Sons, Inc., New York, 1955).

⁵ *Scott's Standard Methods of Chemical Analysis*, edited by N. H. Furman (D. Van Nostrand, Inc., Princeton, New Jersey, 1959) 5th ed., Vol. I.

⁶ J. Kleinberg, LA-1721 (September 1954), Los Alamos Report, LA-1721 (September 1954) (unpublished).

⁷ K. A. Krauss and F. Nelson, *Proceedings of the International*

TABLE I. (*d,p*) activation cross sections.

Target	Target material	Product	$T_{1/2}$	Incident deuteron energy (MeV)	σ (mb)
$^{11}\text{Na}_{12}^{23}$	NaCl	$^{11}\text{Na}_{13}^{24}$	15 h	17.0	47.3
$^{19}\text{K}_{22}^{41}$	KI	$^{19}\text{K}_{23}^{42}$	12.5 h	19.5	77.9
$^{25}\text{Mn}_{30}^{55}$	MnO ₂	$^{25}\text{Mn}_{31}^{56}$	2.6 h	18.4	77.6
$^{30}\text{Zn}_{38}^{68}$	ZnO	$^{30}\text{Zn}_{39}^{69m}$	13.8 h	18.0	37.0
$^{31}\text{Ga}_{40}^{71}$	Ga ₂ O ₃	$^{31}\text{Ga}_{41}^{72}$	14.3 h	18.8	100.0
$^{33}\text{As}_{42}^{75}$	As ₂ O ₃	$^{33}\text{As}_{43}^{76}$	26.4 h	19.0	76.9
$^{35}\text{Br}_{46}^{81}$	KBr	$^{35}\text{Br}_{47}^{82}$	36 h	18.8	67.4
$^{39}\text{Y}_{50}^{89}$	Y ₂ O ₃	$^{39}\text{Y}_{51}^{90}$	64 h	19.5	103.0
$^{52}\text{Te}_{78}^{130}$	Te	$^{52}\text{Te}_{79}^{131m}$	30 h	19.8	64.3
$^{55}\text{Cs}_{78}^{133}$	CsCl	$^{55}\text{Cs}_{79}^{134m}$	3.2 h	19.4	36.5
$^{56}\text{Ba}_{82}^{138}$	BaO ₂	$^{56}\text{Ba}_{83}^{139}$	84 min	20.0	97.7
$^{57}\text{La}_{82}^{139}$	La ₂ O ₃	$^{57}\text{La}_{83}^{140}$	40.2 h	20.3	100.0
$^{58}\text{Ce}_{84}^{142}$	CeO ₂	$^{58}\text{Ce}_{85}^{143}$	33 h	20.3	101.0
$^{59}\text{Pr}_{83}^{141}$	PrO ₂	$^{59}\text{Pr}_{83}^{142}$	19.1 h	19.7	189.0
$^{67}\text{Ho}_{98}^{165}$	Ho ₂ O ₃	$^{67}\text{Ho}_{99}^{166}$	27.3 h	19.9	100
$^{74}\text{W}_{112}^{186}$	WO ₃	$^{74}\text{W}_{113}^{187}$	24 h	20.0	93.7
$^{79}\text{Au}_{118}^{197}$	Au	$^{79}\text{Au}_{119}^{198}$	67 h	20.3	135
$^{82}\text{Pb}_{126}^{208}$	PbO ₂	$^{82}\text{Pb}_{127}^{209}$	3.3 h	20.3	120

The activated samples were generally less than 5 mg/cm² thick and were prepared for counting with the aid of a filter tower which provided a well defined and always reproducible deposit geometry. The filter paper containing the precipitate was then mounted on a $\frac{1}{16}$ -in.-thick aluminium card, thus guaranteeing saturation back scattering, and covered by 1.82 mg/cm² Saran wrap.

The conversion electron contribution to the measured activities was generally no greater than a few percent, except for the $\text{In}^{115}(d,d'\gamma)$ reaction, and was accounted for when making the usual counting corrections for absorption, back-scattering, and self-absorption.

All target materials used were of natural isotopic composition. Those available in powder, rather than in foil, form were manufactured by a method similar in principle to that reported by Fodor and Cohen,¹⁷ but different in detail. The powder was suspended in a solution of acetone in which has been dissolved some Duco cement which acts as the adhesive for holding the powder to an aluminum backing 4.4 mg/cm² thick. The

Conference on the Peaceful Uses of Atomic Energy (United Nations, New York, 1956), Vol. 7, p. 113.

⁸ M. Lindner, University of California Radiation Laboratory Report UCRL-4377, 1954 (unpublished).

⁹ W. J. Maeck, M. E. Kussy, and J. E. Rein, *Anal. Chem.* **33**, 237 (1960).

¹⁰ S. K. Majumdar and A. K. De, *Anal. Chem.* **33**, 297 (1961).

¹¹ W. W. Meinke, Atomic Energy Commission Declassified Report, AEC-D-2788 (August 1949) (unpublished).

¹² *Analytical Chemistry of the Manhattan Project*, edited by C. J. Rodden (McGraw-Hill Book Company, Inc., New York, 1950), Vol. VIII-1.

¹³ E. M. Scadden and N. E. Ballow, NAS-NS3009 (January 1960), National Academy of Science Report (unpublished).

¹⁴ E. P. Steinberg, NAS-NS3011 (January 1960), National Academy of Science Report (unpublished).

¹⁵ P. C. Stevenson and N. E. Nervik, NAS-NS3020 (February 1961), National Academy of Science Report (unpublished).

¹⁶ A. P. Vogel, *A Textbook of Quantitative Inorganic Analysis* (Longman's Green and Company, Inc., New York, 1959).

¹⁷ G. Fodor and B. L. Cohen, *Rev. Sci. Instr.* **31**, 73 (1960).

TABLE II. (*d,t*) activation cross sections.

Target	Target material	Product	$T_{1/2}$	Incident deuteron energy (MeV)	σ (mb)
$^{28}\text{Ni}_{30}^{58}$	Ni	$^{28}\text{Ni}_{29}^{57}$	36 h	18.8	6.1
$^{33}\text{As}_{42}^{75}$	As ₂ O ₃	$^{33}\text{As}_{41}^{74}$	18 days	19.2	15.7
$^{40}\text{Zr}_{50}^{90}$	ZrO ₂	$^{40}\text{Zr}_{49}^{89}$	79 h	19.0	17.9
$^{53}\text{I}_{74}^{127}$	KI	$^{53}\text{I}_{73}^{126}$	13.3 days	20.0	29.0
$^{79}\text{Au}_{118}^{197}$	Au	$^{79}\text{Au}_{117}^{196}$	5.6 days	20.3	49.5

Duco cement consists of hydrogen, carbon, nitrogen, and oxygen nuclei for which no reaction products will be formed having half-lives as long as the shortest detected in this work. Preparatory to mounting the activated sample for counting, the Duco cement was removed in an acetone bath thus separating the powder from its aluminum backing and allowing a measurement of the true target weight. In general, target thicknesses were between 3 and 5 mg/cm², and the Duco cement typically accounted for between 5 and 8% of the uncorrected target weight. Care was taken not to use targets weighing less than 3 mg/cm² since the Duco cement contribution increases rapidly for smaller target weights. For carrier-free activated samples, the target weight error due to the Duco cement is of no consequence since the correction does not enter into the activity calculation. Since more than 50% of the target area was exposed to the deuteron beam, the effective thickness of the irradiated portion of the target should be very close to the average thickness for the total target area. Target cooling was achieved by stacking the targets $\frac{1}{4}$ in. apart and forcing air through these spaces.

RESULTS AND ANALYSIS

There are 47 deuteron-induced activation cross sections listed in Tables I, II, III, IV, and V. These cross sections are estimated to have an experimental uncertainty of less than 15% and have been confirmed by at least two, and in some cases three or more, independent measurements.

TABLE III. (*d,2p*) activation cross sections

Target	Target material	Product	$T_{1/2}$	Incident deuteron energy (MeV)	σ (mb)
$^{16}\text{S}_{16}^{32}$	S	$^{16}\text{P}_{17}^{32}$	14.2 days	18.3	139
$^{26}\text{Fe}_{30}^{56}$	Fe	$^{26}\text{Mn}_{31}^{56}$	2.6 h	19.1	14.6
$^{27}\text{Co}_{32}^{59}$	Co ₃ O ₄	$^{26}\text{Fe}_{33}^{59}$	45 days	19.5	10.3
$^{29}\text{Cu}_{36}^{65}$	Cu	$^{28}\text{Ni}_{37}^{65}$	2.6 h	19.4	0.820
$^{33}\text{As}_{42}^{75}$	As ₂ O ₃	$^{32}\text{Ge}_{43}^{75}$	82 min	18.9	0.157
$^{39}\text{Y}_{50}^{89}$	Y ₂ O ₃	$^{38}\text{Sr}_{51}^{89}$	51 days	19.9	0.336
$^{47}\text{Ag}_{62}^{109}$	Ag	$^{46}\text{Pd}_{63}^{109}$	13.5 h	19.7	0.0235
$^{53}\text{I}_{74}^{127}$	KI	$^{52}\text{Te}_{75}^{127}$	9.4 h	20.0	0.0140

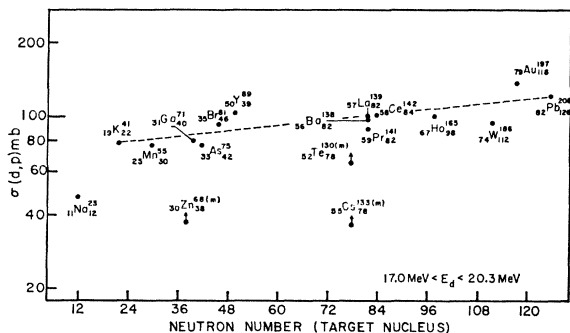
TABLE IV. $(d,p\alpha) + (d,\alpha p)$ activation cross sections.

Target	Target material	Product	$T_{1/2}$	Incident deuteron energy (MeV)	σ (mb)
$^{17}\text{Cl}_{18}^{35}$	NaCl	$^{15}\text{P}_{17}^{32}$	14.2 days	18.6	72.6
$^{27}\text{Co}_{32}^{59}$	Co_2O_4	$^{25}\text{Mn}_{31}^{56}$	2.6 h	19.1	3.84
$^{28}\text{Ni}_{34}^{62}$	Ni	$^{26}\text{Fe}_{33}^{59}$	45 days	17.4	1.35
$^{30}\text{Zn}_{38}^{68}$	ZnO	$^{28}\text{Ni}_{37}^{65}$	2.6 h	18.2	0.119
$^{33}\text{As}_{42}^{75}$	As_2O_3	$^{31}\text{Ga}_{41}^{72}$	14.3 h	19.4	0.219
$^{35}\text{Br}_{44}^{79}$	KBr	$^{33}\text{As}_{43}^{76}$	26.4 h	18.9	0.201
$^{49}\text{In}_{66}^{115}$	In	$^{47}\text{Ag}_{65}^{112}$	3.2 h	19.3	0.053
$^{57}\text{La}_{82}^{139}$	La_2O_3	$^{55}\text{Cs}_{81}^{136}$	13 days	20.3	0.071

A. (d,p) Reactions

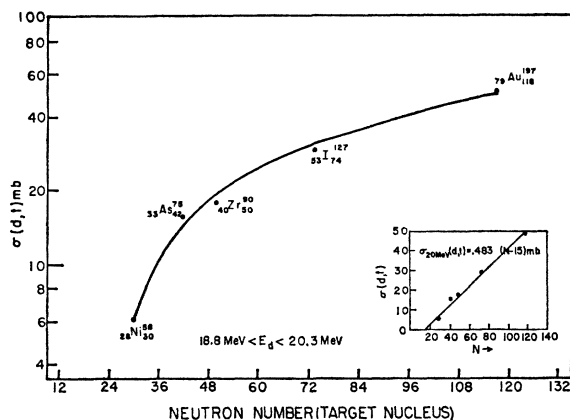
The (d,p) activation cross sections, listed in Table I and pictured in Fig. 1, represent the activation cross sections determined from the decay of the ground state of the residual nucleus in every case except the three low-lying values of Zn, Te, and Cs. These cross sections are determined from the decay of an isomeric level of the residual nucleus; the first excited states of Zn^{69} and Te^{131} , and the second excited state of Cs^{134} . Inspection of this data reveals the striking feature that these cross sections as a function of neutron number cluster about a slowly and monotonically increasing curve from 48 mb for K^{41} to 120 mb for Pb^{208} . It is not too meaningful to ascribe reasons for the slight deviations from a smooth variation because of the 15% experimental uncertainties.

Since (d,p) reactions are known to proceed principally by a stripping process, it is interesting to compare the best theoretical prediction of such a mechanism with the experimental value of the (d,p) activation cross section. Accordingly, a distorted-wave Born approximation calculation¹⁸ was performed for the reaction $\text{Ni}^{58}(d,p)\text{Ni}^{59}$. This reaction was chosen since the centroids of the single-particle states, and their spectroscopic factors, were experimentally well determined from previous studies.¹⁹ The contribution of each level

FIG. 1. Activation cross sections for (d,p) reactions.

¹⁸ R. H. Bassel, R. M. Drisko, and G. R. Satchler, Oak Ridge National Laboratory ORNL-3240, 1962 (unpublished).

¹⁹ B. L. Cohen, R. H. Fulmer, and A. L. McCarthy, Phys. Rev. **126**, 698 (1962).

FIG. 2. Activation cross sections for (d,t) reactions.

to the stripping cross section is listed in Table VI. The optical model potentials listed in Table VI for the incident deuterons were interpolated from the 15 MeV data of Melkanoff²⁰ and the 19.5-MeV data of Hodgson *et al.*²¹ The optical model potentials listed in Table VI for the outgoing particles were obtained from the following expressions which were suggested by the work of Rost²²;

$$V = 50 \text{ MeV} - \frac{1}{2} E$$

and

$$W = 4 \text{ MeV} + \frac{1}{4} E,$$

where E is the kinetic energy of the outgoing particles, in MeV.

For 18.8-MeV incident deuterons, the prediction of the total contribution of (d,p) stripping reactions to the bound levels is seen in Table VI to be 70 mb. Probably the $2d_{3/2}$ level should be included in Table VI, even though it was not detected in the stripping study of Cohen *et al.*¹⁹ The regularity of these cross sections, as pictured in Fig. 1, allows one to assume an activating cross section for Ni^{58} similar to those of neighboring nuclei. Thus, the inclusion of the $2d_{3/2}$ level would

TABLE V. Other activation cross sections.

Reaction	Target	Target material	Product	$T_{1/2}$	Incident deuteron energy (MeV)	σ (mb)
$(d,d'\gamma)$	$^{49}\text{In}_{66}^{115}$	In	$^{49}\text{In}_{66}^{115m}$	4.5 h	19.8	49.5
$(d,2n)$	$^{31}\text{Ga}_{33}^{69}$	Ga_2O_3	$^{32}\text{Ge}_{37}^{69}$	40 h	18.8	717.0
$(d,2n)$	$^{39}\text{Y}_{50}^{89}$	Y_2O_3	$^{40}\text{Zr}_{48}^{89}$	79 h	19.5	838.0
(d,α)	$^{24}\text{Cr}_{26}^{50}$	Cr	$^{23}\text{V}_{25}^{48}$	16 days	18.7	11.3
(d,α)	$^{28}\text{Fe}_{28}^{54}$	Fe	$^{25}\text{Mn}_{27}^{57}$	5.6 days	19.4	12.2
$(d,2pn)$	$^{58}\text{Ce}_{84}^{142}$	CeO_2	$^{57}\text{La}_{84}^{141}$	3.8 h	20.3	20.4
$(d,n\alpha)$	$^{28}\text{Ni}_{30}^{58}$	Ni	$^{27}\text{Co}_{28}^{55}$	18 h	18.8	23.2
$(d,n\alpha)$	$^{30}\text{Zn}_{44}^{64}$	ZnO	$^{29}\text{Cu}_{32}^{61}$	3.3 h	18.0	28.6

²⁰ H. M. Melkanoff, Florida State University Studies **32**, 215 (1959).

²¹ P. E. Hodgson, J. Aguilar, A. García, and J. B. A. England, Nucl. Phys. **22**, 138 (1961).

²² E. Rost, Ph.D. thesis, University of Pittsburgh, 1961 (unpublished).

TABLE VI. Results of distorted-wave Born approximation calculation for the reaction ${}^{28}\text{Ni}_{30}{}^{58}(d,p){}^{28}\text{Ni}_{31}{}^{59}$ induced by 18.8-MeV incident deuterons.

Level	Excitation energy (MeV)	V_d (MeV)	W_d (MeV)	V_p (MeV)	W_p (MeV)	$2l_f+1$	$P(l_n, Q)$	S	σ (mb)
$3s_{1/2}$	7.8	39.3	13.3	41.1	8.45	2	2.54	1.0	5.1
$2d_{5/2}$	5.7			40.1	8.98	6	4.63	1.0	27.8
$1g_{3/2}$	3.0			38.7	9.65	10	1.87	1.0	18.7
$2p_{1/2}$	1.7			38.1	9.98	2	2.66	1.0	5.3
$1f_{5/2}$	0.7			37.5	10.2	6	1.27	0.89	6.8
$2p_{3/2}$	0			37.2	10.4	4	2.21	0.75	6.6
									Total=70.3

further improve agreement with the experimentally determined value in the Ni region, which is seen to be 77 mb for the $\text{Mn}^{55}(d,p)\text{Mn}^{56}$ reaction involving the same neutron numbers as the Ni^{58} reaction. It is concluded that the (d,p) activation cross sections are almost entirely of the direct, stripping type and are closely predicted by the distorted-wave theory of direct nuclear reactions.

B. (d,t) Reactions

The (d,t) activation cross sections, listed in Table II and pictured in Fig. 2, represent in each case the activa-

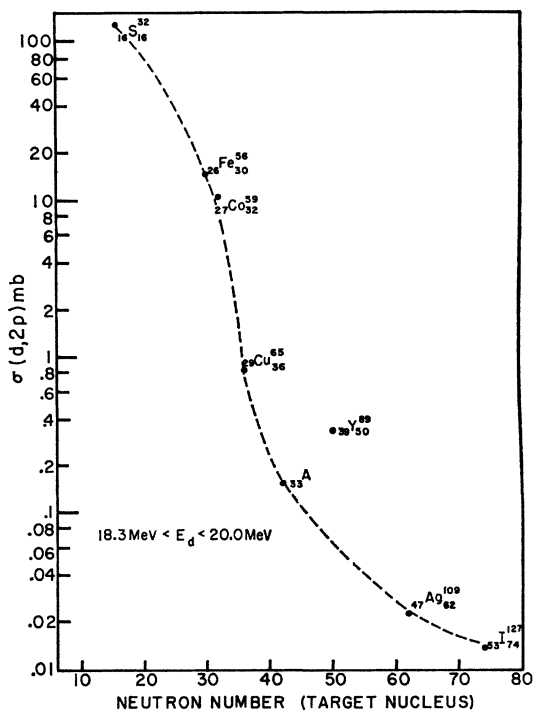


FIG. 3. Activation cross sections for $(d,2p)$ reactions.

tion cross section determined from the decay of the ground state of the residual nucleus. If these cross sections are plotted on a linear scale as a function of neutron number, they fall surprisingly close to a straight line. The equation of this line, which allows an approximate (d,t) activation cross section prediction for about 20-MeV incident deuterons is given as

$$\sigma(d,t) = 0.48(N - 15) \text{ mb.}$$

It is well established from studies of angular distributions and energy spectra of the tritons that (d,t) reactions proceed essentially exclusively by neutron pickup. The fact that the cross section increases monotonically with increasing A (Fig. 2) indicates that Coulomb barriers have little influence in these reactions. Apparently the deuteron is joined by the neutron (to form a triton) far outside of the nucleus.

C. $(d,2p)$ Reactions

The $(d,2p)$ activation cross sections, listed in Table III and pictured in Fig. 3, represent the activation cross sections determined from the decay of the ground state of the residual nucleus. Since these cross sections decrease very rapidly with increasing mass number, a test for the reaction mechanism was made assuming the incident deuteron forms a compound system with the target nucleus, followed by the evaporation of two protons as determined by the statistical theory of nuclear reactions.²³

A computer program was written to perform these calculations on an IBM 7070 Digital Computer at the University of Pittsburgh. This program allows up to two-particle evaporation with three particle channels open for each evaporation; the competition being between alphas, protons, and neutrons. The possibility of gamma emission in competition with particle emission has been ignored in this program. Thus, the expression for calculating the cross section for evaporation of two particles b and e , in that sequence, is written as

$$\sigma(x, be) = \frac{\sigma_C(x) \int_0^{\epsilon_{b \max}} g_b m_b \epsilon \sigma_C(\epsilon) \omega(\epsilon_{b \max} - \epsilon) [F_e/F_e + F_f + F_g] d\epsilon}{F_b + F_c + F_d}, \tag{1}$$

²³ J. M. Blatt and V. F. Weisskopf, *Theoretical Nuclear Physics* (John Wiley & Sons., Inc., New York, 1952).

TABLE VII. ($d,2p$) level density parameters. Column (1) gives the results for the statistical theory. Column (2) gives the statistical theory results if third-particle emission is ignored. Column (3) gives the level density parameter if the process is assumed to be stripping plus evaporation of a second proton. Column (4) gives the results if the processes considered in columns (1) and (3) are both assumed to be present. The ratio of stripping to compound nucleus in the emission of the first proton is listed in column (5).

Target nucleus	Level density parameter (MeV ⁻¹)				(5) Stripping (Comp. nuc.)
	(1)	(2)	(3)	(4)	
Fe ⁵⁶	~1.5	~0.5
Co ⁵⁹	~1.5	~0.5
Cu ⁶⁵	4.1	4.8	4.2	5.7	1.1
As ⁷⁵	9.4	12.4	12.5	13.6	2.7
Y ⁸⁹	4.5	4.8	5.8	6.8	1.8
Ag ¹⁰⁹	5.0	8.0	7.0	7.5	3.2
I ¹²⁷	4.7	9.5	6.5	6.9	3.6

where particles c and d compete with b for first-particle emission and particles f and g compete with e for second-particle emission. In expression (1), m and ϵ are the outgoing channel mass and energy, g_b is the spin degeneracy of particle b , $\omega(\epsilon_{b\max} - \epsilon)$ is the level density of the residual nucleus which can be written as

$$\omega = \text{const} \exp\{2[a(\epsilon_{b\max} - \epsilon)]^{1/2}\}, \quad (2)$$

where a is the level density parameter as defined by Blatt and Weisskopf,²³ $\sigma_C(\epsilon)$ is the cross section for formation of a compound nucleus, and the term F_k is the integrated spectrum of the outgoing k particles which is written as

$$F_k = \int_0^{\epsilon_{k\max}} g_k m_k \epsilon \sigma_C(\epsilon) \omega(\epsilon_{k\max} - \epsilon) d\epsilon. \quad (3)$$

The cross sections for formation of compound nuclei by incident alphas, protons, deuterons, and neutrons, were obtained from the continuum theory calculations of Shapiro²⁴ and Blatt and Weisskopf,²³ and are permanent data inventory. The program performs a logarithmic two-dimensional parabolic interpolation to obtain the needed compound cross sections at any energy and atomic number. In addition, the program allows a pairing energy reduction of the excitation energy of the residual nucleus in Eq. (2) and in the integration limits of Eqs. (1) and (3) by $\delta_p + \delta_n$ where

$$\epsilon_{k\max} \rightarrow \epsilon_{k\max} - \delta_p - \delta_n.$$

The pairing energies used were those of Cameron.²⁵

The calculation results include the activation cross section which is determined during the calculation of the total cross section by ignoring those terms in the numerical integration of the final-particle spectrum for which the residual nucleus has an excitation energy large enough to result in any additional particle emis-

sion. The program can be instructed to repeat a cross-section calculation for as many as six different level density parameters, and, if requested, an excitation function will be calculated for each level density parameter. The print-out of the above calculation includes the spectra of all outgoing particles as well as the F values given by Eq. (3).

In these calculations, the value of the nuclear radius was determined from

$$R = r_0 A^{1/3} \times 10^{-13} \text{ cm}$$

for incident protons and neutrons, and

$$R = (r_0 A^{1/3} + 1.21) \times 10^{-13} \text{ cm}$$

for incident alphas and deuterons, where r_0 was chosen to be 1.6.

The level density parameters required to give the observed ($d,2p$) activation cross sections are listed in Table VII. In column (2) of Table VII are listed for comparison the parameters predicted by statistical theory when third particle emission is ignored. The large reaction Q values available for third-particle alpha emission following the ($d,2p$) reactions on Ag¹⁰⁹ and I¹²⁷ result in a significant decrease in the level density parameters which are needed to account for the observed ($d,2p$) activation cross sections for these two reactions. Since these calculations neglected the possibility of gamma emission in competition with particle emission, it is possible that the level density parameter reduction necessitated by third particle alpha emission is not so drastic as listed in Table VII.

For S³², the statistical theory gives only a very slight dependence of $\sigma(d,2p)$ on the level density parameter, so that a determination of the latter has little meaning; the cross section is of about the correct order of magnitude. For Fe⁵⁶ and Co⁵⁹, the observed cross sections are too large to be explained by any level density parameter. However, the cross sections for the five heavier nuclei are readily explainable by the statistical theory with not unreasonable level density parameters.

Two other models for a ($d,2p$) reaction might be considered, firstly one in which one proton is emitted in a direct interaction (i.e., stripping) and the other is evaporated from the residual nucleus, and secondly a model in which both protons are emitted in a direct interaction. A crude estimate of the cross section for the first of these processes may be obtained by assuming that the spectrum of stripping protons is the same as that of first protons from a compound nucleus model, but taking the total cross section for emission of a first proton from stripping theory. A calculation of this type was made with the (d,p) stripping cross section assumed to be 200 mb as roughly estimated from theory. The cross sections calculated from the statistical theory program were then adjusted by the ratio of 200 mb to the cross section for the first emitted particle to be a proton, a quantity readily obtainable as a computer

²⁴ M. A. Shapiro, Phys. Rev. **90**, 171 (1953).

²⁵ A. G. W. Cameron, Can. J. Phys. **36**, 1040 (1958).

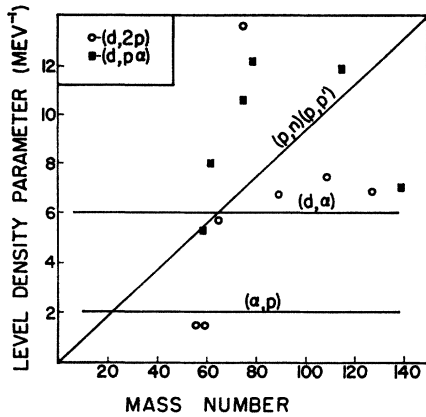


FIG. 4. Level density parameters needed to explain $(d,2p)$ and $(d,p\alpha)$ cross sections. The data are from column (4) of Table VII and from column (6) of Table VIII. The lines labeled (p,n) , (p,p') and (α,p) are from reference 26, and the line labeled (d,α) is meant to represent the data of reference 27.

print out. The resulting level density parameters needed to fit the observed cross sections are shown in column (3) of Table VII.

Actually, one expects both a compound nucleus process and a stripping plus evaporation process. Since the above calculation gives the ratio between the two, the observed cross section can be divided between the two processes in this ratio. The level density parameters then needed to explain the observed cross sections are listed in column (4) of Table VII. The estimated ratio of stripping to compound nucleus is listed in column (5).

The level density parameters from column (4) of Table VII are plotted vs A in Fig. 4. Figure 4 also shows the values of the level density parameter found in other types of experiments.²⁶⁻²⁸ In view of the wide variation of the latter, the results found here cannot be considered unacceptable. On the other hand, the principal sensitivity in these experiments is in the evaporation of the second proton, and previous experiments of this type have usually given large level density parameters.²⁶ In this sense, the level density parameters found here are unexpectedly small. This is most certainly true in the cases of Fe^{56} and Co^{59} . This may be an indication that a process in which both protons are emitted in a direct interaction is present to some extent.

D. $(d,p\alpha)$ and $(d,\alpha p)$ Reactions

The $(d,p\alpha) + (d,\alpha p)$ activation cross sections, listed in Table IV and plotted vs N in Fig. 5, represent the activation cross sections determined from the decay of the ground state of the residual nucleus. An analysis similar to that described above for $(d,2p)$ reactions was carried out. Listed in columns (1) and (2) of Table VIII are the level density parameters required to explain the

TABLE VIII. $(d,p\alpha)$ and $(d,\alpha p)$ level density parameters. Column (1): $(d,\alpha p)$ by compound nucleus process. Column (2): same neglecting third-particle emission. Column (3): $(d,p\alpha)$ by compound nucleus process. Column (4): same neglecting third-particle emission. Column (5): $(d,p\alpha)$ by stripping followed by alpha-particle evaporation. Column (6): Combination of processes in columns (3) and (6). The ratio of stripping to compound nucleus in the emission of the proton assumed in column (6) is listed in column (7).

Target nucleus	$(d,\alpha p)$ level density param. (MeV ⁻¹)		$(d,p\alpha)$ level density parameters (MeV ⁻¹)				(7) $\left(\frac{\text{Stripping}}{\text{Comp. nuc.}}\right)$
	(1)	(2)	(3)	(4)	(5)	(6)	
Cl ³⁵	9.9	12.0	1.0	1.0	
Co ⁵⁹	1.8	1.9	4.0	4.0	4.0	5.2	1.0
Ni ⁶²	6.0	6.0	6.9	8.0	1.5
Zn ⁶⁸	5.1	5.4	<i>a</i>	<i>a</i>	<i>a</i>	<i>a</i>	<i>a</i>
As ⁷⁵	6.1	6.5	7.9	8.1	9.5	10.5	2.2
Br ⁷⁹	7.7	7.9	9.3	9.4	10.6	12.1	1.7
In ¹¹⁵	1.2	1.3	7.9	8.0	11.6	11.8	10.0
La ¹³⁹	1.5	1.7	4.4	4.4	7.0	7.0	12.7

* Insufficient information available on Q values.

observed cross sections if the reactions proceed by evaporation of an alpha particle from a compound nucleus followed by evaporation of a proton from the residual nucleus. Since a compound nucleus process has been shown²⁷ to be predominant in (d,α) reactions except in the uppermost few MeV of the alpha spectrum, no consideration need be given to the possibility that a $(d,\alpha p)$ reaction proceeds by a (d,α) direct interaction followed by proton evaporation.

It is also necessary to consider $(d,p\alpha)$ reactions as a source of the activities observed. Calculations com-

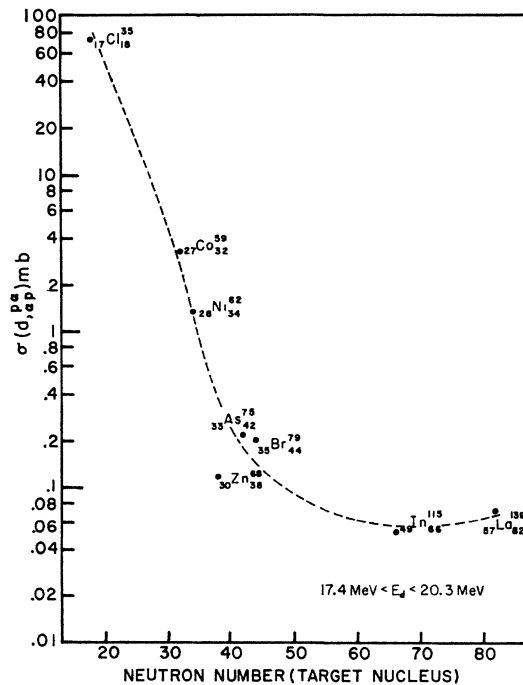


FIG. 5. Activation cross sections for $(d,p\alpha) + (d,\alpha p)$ reactions.

²⁶ C. Igo and H. E. Wegner, Phys. Rev. **102**, 1364 (1956).
²⁷ J. B. Mead and B. L. Cohen, Phys. Rev. **125**, 947 (1962).
²⁸ L. W. Swenson and N. Cindro, Bull. Am. Phys. Soc. **5**, 76 (1960).

pletely analogous to those described above in connection with $(d,2p)$ reactions were carried out. There is some difficulty in the fact that very low energy alpha-particle emission might not compete favorably with gamma emission in heavy nuclei. However, this effect was studied and found not to be an appreciable source of error.

The results of the calculations on $(d,p\alpha)$ reactions are shown in Table VIII, columns (3)–(6). Listed there are the level density parameters needed to explain the observed cross sections assuming a compound nucleus process, column (3); a compound nucleus process neglecting third particle emission, column (4); a (d,p) stripping reaction followed by evaporation of an alpha particle, column (5); and a combination of the two processes considered in columns (3) and (5), column (6). The ratios of stripping to compound nucleus cross sections used in obtaining columns (5) and (6) are listed in column (7).

The first question to decide is whether $(d,p\alpha)$ or $(d,\alpha p)$ is the predominant process. The one requiring the larger level density parameter has the larger cross section since, if the other reaction had that large a level density parameter, its cross section would be smaller. An inspection of Table VIII reveals that $(d,\alpha p)$ is the predominant process in Cl^{35} , but that $(d,p\alpha)$ is predominant in all other cases. In fact, the predominances are always sufficiently strong that the alternative process may be ignored.

The level density parameters from column (6) of Table VIII are shown in Fig. 4. They are in rather good agreement with the results of other experiments. Thus, the reaction mechanism in these reactions is not open to serious question on the basis of these results.

E. Other Reactions

The activation cross sections listed in Table V were determined from the decay of the ground state of the residual nucleus in every case except, of course, the $(d,d'\gamma)$ reaction on In^{115} . The cross section for the $\text{In}^{115}(d,d'\gamma)$ reaction is in good agreement with the value reported by Porile²⁹ whose analysis indicates emission of a proton and neutron rather than a deuteron. From the work of Hamburger *et al.*³⁰ the (d,pn) cross sections are expected to be several hundred millibarns. The

²⁹ N. T. Porile, Phys. Rev. **121**, 184 (1961).

³⁰ E. W. Hamburger, B. L. Cohen, and R. E. Price, Phys. Rev. **121**, 1143 (1961).

fact that only a small percentage goes to the isomer is in general agreement with studies of isomeric cross section ratios³¹ which show, at these energies, that the reaction to the high-spin state predominates.

The $(d,2n)$ activation cross sections for Ga^{69} and Y^{89} are about 720 mb and 840 mb, respectively, which is well over half of the expected total reaction cross section and much larger than (d,pn) cross sections in this mass region even including cases (accounting for the largest part) where the latter reaction takes place via deuteron break-up by the Coulomb and nuclear potentials far outside the nucleus.³⁰ This indicates that low-energy neutrons are far more numerous than low-energy protons, which indicates that compound nucleus formation rather than stripping is the predominant reaction when deuterons bombard nuclei in this mass region.

The (d,α) cross sections are difficult to interpret as they were shown by Mead *et al.*²⁷ to result partially from direct as well as compound nucleus processes.

The $\text{Ce}^{142}(d,2pn)$ cross section is probably not a (d,He^3) reaction because of unfavorable energy considerations. The (d,He^3) reactions studied by Cujec³² using 15-MeV incident deuterons are seen to have small cross sections in light nuclei, rapidly decreasing with increasing A , and no measurable cross section above Cu. It is possible that the reaction proceeds by $(d,d'p)$ which is energetically more favorable.

Cross sections for $(d,n\alpha)$ on Ni^{58} and Zn^{64} are an order of magnitude larger than for $(d,p\alpha)$ in the same mass region; this again indicates that compound nucleus is the predominant process in determining the low-energy part of the spectrum of the first emitted particle.

ACKNOWLEDGMENTS

The authors wish to express their appreciation to Dr. James Blue and his staff at the Lewis Research Center Cyclotron of the National Aeronautics and Space Administration in Cleveland, Ohio for permission to use their accelerator. Also, special recognition is extended to James Christman for his assistance in the radiochemical separations.

The authors also wish to thank Dr. A. J. Allen and acknowledge the financial support given by the Office of Naval Research and the National Science Foundation.

³¹ C. T. Bishop, Argonne National Laboratory ANL-6405, 1961 (unpublished).

³² B. Cujec (private communication).